

Spin-polarized tunneling in hybrid metal-semiconductor magnetic tunnel junctions

S. H. Chun,* S. J. Potashnik, K. C. Ku, P. Schiffer, and N. Samarth[†]

Department of Physics and Materials Research Institute, The Pennsylvania State University, University Park, Pennsylvania 16802

(Received 1 July 2002; published 30 September 2002)

We demonstrate efficient spin-polarized tunneling between a ferromagnetic metal and a ferromagnetic semiconductor with highly mismatched conductivities. This is indicated by a large tunneling magnetoresistance (up to 30%) at low temperatures in epitaxial magnetic tunnel junctions composed of a ferromagnetic metal (MnAs) and a ferromagnetic semiconductor ($\text{Ga}_{1-x}\text{Mn}_x\text{As}$) separated by a nonmagnetic semiconductor (AlAs). Analysis of the current-voltage characteristics yields detailed information about the asymmetric tunnel barrier. The low temperature conductance-voltage characteristics show a zero bias anomaly and a \sqrt{V} dependence of the conductance, suggesting a correlation gap in the density of states of $\text{Ga}_{1-x}\text{Mn}_x\text{As}$. These experiments suggest that MnAs/AlAs heterostructures offer well characterized tunnel junctions for high efficiency spin injection into GaAs.

DOI: 10.1103/PhysRevB.66.100408

PACS number(s): 72.25.Mk, 73.40.Gk

Fundamental studies of spin-dependent transport and tunneling in metallic ferromagnetic heterostructures have been of critical importance to the development of metallic “spintronic” devices for high density information storage.¹ The emerging interest in a *semiconductor*-based “spintronics” technology has now sparked substantial interest in studies of similar phenomena in semiconductor heterostructures.² An important hurdle in this context is the inefficient injection of spin-polarized currents from metallic ferromagnets into semiconductors due to the large mismatch in conductivities.³ This problem can be overcome by using either ferromagnetic semiconductors or highly spin-polarized paramagnetic semiconductors for spin injection.⁴ Alternatively, spins can be injected from a ferromagnetic metal via a tunnel barrier,⁵ and the conductivity mismatch problem is essentially circumvented by the large contact resistance.⁶ A direct scheme for detecting spin injection in this case is to measure the tunneling magnetoresistance (TMR) between metallic ferromagnetic tunnel contacts that sandwich a semiconductor;⁶ one tunnel barrier serves as a spin injector and the other a spin detector, and the physics is completely analogous to that of a traditional magnetic tunnel junction (MTJ).⁷ The fabrication of high quality epitaxial metal/semiconductor/metal heterostructures needed for such a scheme presents a difficult materials challenge. For instance, even in the most successful examples of such epitaxial MTJ’s (MnAs/AlAs/MnAs), the magnetoresistance effects are small ($\approx 1\%$).⁸

Here we demonstrate efficient spin-polarized tunneling in a class of “hybrid” epitaxial MTJ’s comprised of a ferromagnetic metal (MnAs) and a ferromagnetic semiconductor ($\text{Ga}_{1-x}\text{Mn}_x\text{As}$) separated by a nonmagnetic semiconductor (AlAs). Although the current experiment is limited to detecting spin injection at temperatures below the relatively low Curie temperature of $\text{Ga}_{1-x}\text{Mn}_x\text{As}$ ($T_C=70$ K), the high Curie temperature of MnAs ($T_C=320$ K) allows for future room temperature experiments in different configurations. We note the low Curie temperature of the $\text{Ga}_{1-x}\text{Mn}_x\text{As}$ layer provides a built-in control experiment since we can measure the TMR in both the paramagnetic and ferromagnetic states of $\text{Ga}_{1-x}\text{Mn}_x\text{As}$. Unlike traditional MTJ’s based upon metallic ferromagnets,⁷ or the recently developed all-

ferromagnetic semiconductor MTJ’s wherein the ferromagnetic layers have comparable conductivities,⁹ the ferromagnetic components in our hybrid heterostructures have conductivities differing by four orders of magnitude ($\approx 1 \mu\Omega \text{ cm}$ for MnAs and $\approx 10 \text{ m}\Omega \text{ cm}$ for $\text{Ga}_{1-x}\text{Mn}_x\text{As}$).^{10,11} These hybrid systems hence open up a distinct class of devices that could yield interesting insights into the physics of MTJ’s.

Samples are fabricated by molecular-beam epitaxy on p^+ -GaAs(001) substrates after the growth of a 40-nm-thick p -GaAs buffer layer. We have studied a wide variety of sample configurations involving GaAs, (Ga,Mn)As, (Ga,Al)As and MnAs, but focus here on a systematic set of four samples wherein $\text{Ga}_{1-x}\text{Mn}_x\text{As}$ ($x=0.03$, thickness 120 nm), GaAs (thickness 1 nm), AlAs (thickness $d_{\text{AlAs}}=1, 2, 5$, and 10 nm), GaAs (thickness 1 nm), and MnAs (thickness 45 nm) are grown sequentially at 250 °C. The thin GaAs spacer layers placed between the ferromagnetic layers and the tunnel barrier seem crucial to the observation of distinct TMR characteristics.⁹ Reflection high energy electron diffraction measurements during the growth confirm the epitaxy of MnAs in the “type-B” orientation.¹² Photolithography and wet-etching techniques define 300- μm -diameter mesas etched down into the p -GaAs region for vertical transport measurements. The dc current-voltage characteristics of a mesa between the top MnAs layer and the back of the p -GaAs substrate are measured using a four-probe method in a continuous flow He cryostat over the range 4.2–300 K with an in-plane magnetic field ranging up to 2 kG provided by an electromagnet; additional transport measurements down to 330 mK use a He 3 cryostat with a superconducting magnet. Finally, magnetization is measured on 10-mm² pieces of the unpatterned wafer using a Quantum Design superconducting quantum interference device magnetometer.

Figure 1(a) shows the magnetization hysteresis loop measured at 5 K for the sample with an AlAs barrier thickness $d_{\text{AlAs}}=5$ nm. The magnetic field is applied along the easy axis of “type-B” MnAs, parallel to $[1\bar{1}0]$ GaAs.¹² Two distinct transitions at 20 and 500 Oe indicate the switching of magnetization direction of $\text{Ga}_{1-x}\text{Mn}_x\text{As}$ and MnAs, respec-

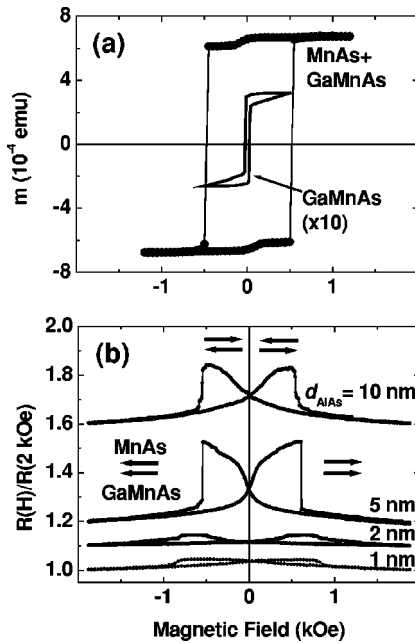


FIG. 1. (a) Magnetic hysteresis loops at $T=5$ K for a MnAs-Ga_{1-x}Mn_xAs hybrid junction and for the same sample after the MnAs layer is removed. The transition of Ga_{1-x}Mn_xAs is broadened by the adjacent MnAs layer. (b) Magnetoresistances of hybrid junctions with a different AlAs barrier thickness ($T=4.2$ K). The curves are shifted for clarity.

tively; the coercive field of the Ga_{1-x}Mn_xAs layer is more readily seen by chemically removing the MnAs layer [see the inset to Fig. 1(a)]. Figure 1(b) shows the TMR for all four samples normalized at the high-field value. A sudden resistance drop accompanies the switching of the MnAs magnetization from antiparallel to parallel with respect to the Ga_{1-x}Mn_xAs magnetization. We note that the TMR shows a nonmonotonic dependence on the AlAs barrier thickness d_{AlAs} , with a striking effect of around 30% for the sample with $d_{\text{AlAs}}=5$ nm.

These results are interpreted in straightforward analogy with metallic MTJ's: the tunneling probability is larger when the two ferromagnetic layers are magnetically aligned than when they are antialigned. Quantitatively, the change in the tunnel resistance is given by¹³

$$T = \frac{(R_A - R_P)}{R_P} = \frac{2P_G P_M}{(1 - P_G P_M)}, \quad (1)$$

where R_A and R_P are the junction resistances with antiparallel and parallel moments, P_G and P_M are the spin polarizations of Ga_{1-x}Mn_xAs and MnAs, respectively. If the spin polarizations P_G and P_M were known, one could estimate the spin injection efficiency through the tunnel barrier as a ratio of the observed TMR to the ideal TMR predicted by the above equation. Direct measurements of P_M and P_G are not yet available, but band structure calculations predict $P_G=1$ for $x \geq 0.125$ and $P_M=0.3$.^{14,15} Assuming that the half-metallicity of Ga_{1-x}Mn_xAs holds down to $x=0.03$ (i.e., $P_G=1$), the TMR observed in our measurements is close to 40% of the ideal TMR. This is a very conservative estimate

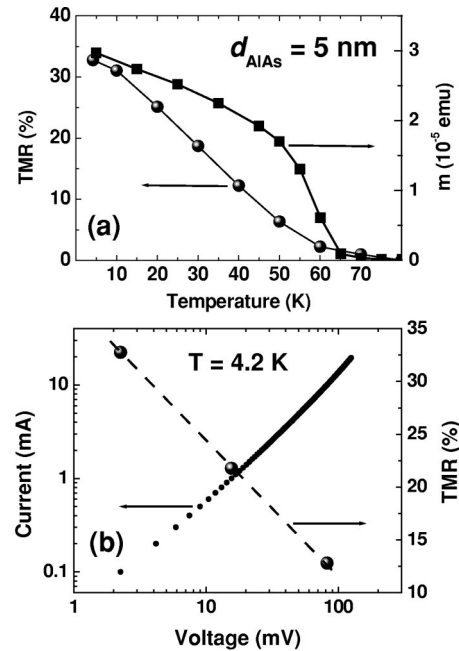


FIG. 2. (a) Temperature dependences of Ga_{1-x}Mn_xAs magnetization at 50 Oe and TMR measured with $I=100 \mu\text{A}$ for a junction with $d_{\text{AlAs}}=5$ nm. (b) I - V characteristics and voltage dependence of TMR for the same junction at 4.2 K.

since the bulk magnetization of Ga_{1-x}Mn_xAs (Ref. 16) is far less than $4\mu_B$ expected for a half-metallic system.¹⁴ Spurious effects that might artificially enhance TMR such as magneto-resistance due to fringe fields can be ruled out in our measurements since the magneto-resistances of the individual MnAs and Ga_{1-x}Mn_xAs layers are smaller than 0.5% for the field range shown in Fig. 1(b). Further, the systematic variation of the TMR with barrier thickness rules out possible effects of fringe fields due to the nearby MnAs layer on Ga_{1-x}Mn_xAs. We now focus on the sample with $d_{\text{AlAs}}=5$ nm in order to examine the physics of these MTJs in some depth.

In contrast with all-metal MTJ's where there is a negligible change in magnetization with temperature, the magnetization and hence the spin-polarization of Ga_{1-x}Mn_xAs depend strongly on temperature. Figure 2(a) shows the temperature dependence of the TMR along with that of the bulk magnetization. Both disappear at the Curie temperature of Ga_{1-x}Mn_xAs (around 70 K). The figure also shows that the temperature dependences of the TMR and the magnetization are quite different. This discrepancy may be related to the faster decay of surface magnetism, as is found in other half-metallic systems,¹⁷ or it may indicate that the spin polarization in Ga_{1-x}Mn_xAs is not directly proportional to the magnetization. The correlation of the TMR with T_C is a unique feature of these junctions where one can probe both ferromagnetic and paramagnetic states by changing the temperature.

The voltage dependence of the TMR at 4.2 K [Fig. 2(b)] shows a rapid decay of the TMR at voltages as low as 100 mV. This qualitatively resembles similar behavior in metallic MTJ's, but the relative scale of the voltage is much smaller

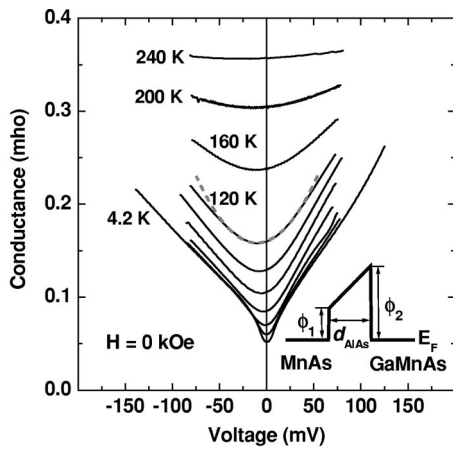


FIG. 3. Zero field conductance curves of the junction used in Fig. 2 at selected temperatures. $T=20,40,60,80$, and 100 K for the curves between 4.2 and 120 K. The dashed line superimposed on the 120 -K data is a fit to Brinkman-Dynes-Rowell model over the range ± 40 mV (see the text). The inset shows the schematic diagram of the model.

in these hybrid MTJ's.⁷ The rapid decrease in the TMR with voltage is likely related to the smaller spin splitting in the $\text{Ga}_{1-x}\text{Mn}_x\text{As}$ layer (≈ 100 meV) compared to typical splittings in metallic ferromagnets (~ 1 eV). Figure 3 shows the G - V characteristics measured at zero magnetic field for several temperatures between 4.2 and 240 K. A distinct zero bias anomaly develops below the T_C of $\text{Ga}_{1-x}\text{Mn}_x\text{As}$, suggesting a small energy gap around the Fermi energy. Another noticeable feature is the asymmetry in the G - V curves: the conductance under positive bias (wherein the MnAs is at a higher potential) is larger than that under negative bias, and—at temperatures above the Curie temperature of $\text{Ga}_{1-x}\text{Mn}_x\text{As}$ —the minimum conductance occurs away from zero bias. A full analysis of the G - V characteristics below the T_C of $\text{Ga}_{1-x}\text{Mn}_x\text{As}$ is not possible because the detailed valence band structure of this material is presently not known from experiment. Instead we focus on the G - V characteristics above T_C where the conductance-voltage curves are parabolic within the voltage range ± 40 mV (see for instance the data for $T \geq 120$ K in Fig. 3).

The asymmetric shape and the occurrence of minimum conductance at a finite voltage lead us to apply the Brinkman-Rowell-Dynes (BDR) tunneling model that was originally developed to calculate the tunneling across metal-insulator-metal junctions with different barrier heights at the interfaces.¹⁸ Although $\text{Ga}_{1-x}\text{Mn}_x\text{As}$ is not a metal, the BDR model is still applicable for voltages less than the Fermi energy of $\text{Ga}_{1-x}\text{Mn}_x\text{As}$ (0.16 eV if we assume a hole density of $1 \times 10^{20} \text{ cm}^{-3}$). A best fit to the BDR model—shown for the data at 120 K in Fig. 3—allows us to extract the barrier heights at the MnAs/AlAs interface (ϕ_1) and the $\text{Ga}_{1-x}\text{Mn}_x\text{As}$ /AlAs interface (ϕ_2), as well as the barrier thickness (d_{AlAs}) (see the inset of Fig. 3).

The best value for ϕ_1 is 0.15 ± 0.01 eV, which is much smaller than that obtained (0.8 eV) in studies of MnAs/AlAs/MnAs MTJ's grown on (111) GaAs.⁸ This discrepancy can be attributed to the different orientation of the MnAs growth

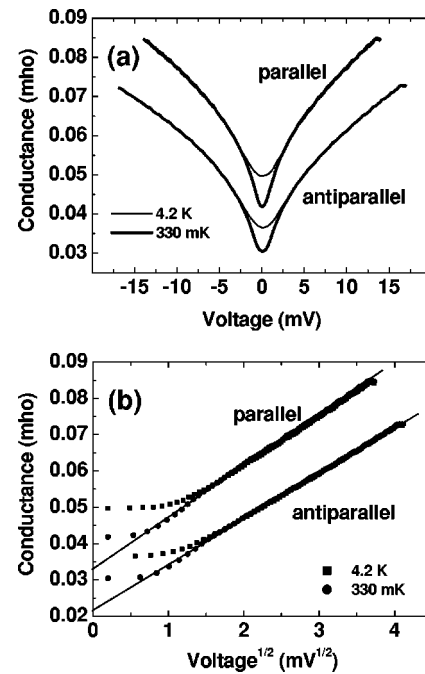


FIG. 4. (a) Low bias conductance curves for the same junction as in Figs. 2 and 3 ($d_{\text{AlAs}}=5$ nm) for parallel and antiparallel magnetization directions. The zero-bias anomaly is more pronounced at 330 mK. (b) The data in (a) are plotted as a function of $V^{1/2}$. Linear fits (solid lines) are used to extract the correlation gap (see the text). The deviation at low bias is due to thermal broadening.

or to a subtle change at the interface.¹⁹ We note that measurements of Fe/GaN/Fe MTJ's grown on (001) GaAs yield a small barrier height (0.11 eV), comparable to our results.²⁰ A simple estimate of ϕ_2 is given by the difference between the known AlAs-GaAs valence band offset (0.55 eV) and the Fermi energy of $\text{Ga}_{1-x}\text{Mn}_x\text{As}$ (0.16 eV). Our result from fitting the data (0.40 ± 0.01 eV) is close to this estimate (0.39 eV). Equally good agreement is found for the barrier thickness: we determine $d_{\text{AlAs}}=6.7 \pm 0.1$ nm assuming light hole states participate in the tunneling through AlAs, while $d_{\text{AlAs}}=4.4 \pm 0.1$ nm assuming heavy holes. A mixture of light and heavy holes may possibly provide a better description of reality, consistent with the designed AlAs thickness (5 nm). The successful application of the BDR model implies that the conduction is indeed due to tunneling processes.

The development of a zero bias anomaly below the Curie temperature of $\text{Ga}_{1-x}\text{Mn}_x\text{As}$ deserves further attention, since it may help in understanding the electronic structure of $\text{Ga}_{1-x}\text{Mn}_x\text{As}$ at the Fermi energy. Figure 4(a) shows the conductance dip in the low bias conductance curves for parallel and antiparallel spin orientations. As expected, the zero bias anomaly becomes more pronounced as the temperature is lowered from 4.2 K to 330 mK. Since $\text{Ga}_{1-x}\text{Mn}_x\text{As}$ is known to exhibit a metal-insulator transition, we analyze the behavior of the conductance-voltage characteristics within the context of early studies of disordered systems with a metal-insulator transition.²¹ On the metallic side of the metal-insulator transition, the one-electron density of states at the Fermi energy [$N(E)$] can be calculated using a scaling model that includes localization, correlation, and screening, and is given by²²

$$N(E) = N(0)[1 + (E/\Delta)^{1/2}], \quad (2)$$

where the correlation gap Δ is a measure of the screening length. As shown in Fig. 4(b), the conductance in the MTJ's studied here is indeed proportional to $V^{1/2}$ except at the lowest bias, where it is affected by thermal broadening.²³ Since the conductance is proportional to $N(E)$, a linear fit to the data in Fig. 4(b) yields $\Delta = 5.7$ and 3.0 meV for parallel and antiparallel configurations, respectively. Surprisingly (and perhaps coincidentally), these values of the correlation gap in $\text{Ga}_{1-x}\text{Mn}_x\text{As}$ are consistent with those extracted from studies of granular aluminum tunnel junctions²⁴ in the regime wherein the Al conductivity is comparable to that of $\text{Ga}_{1-x}\text{Mn}_x\text{As}$.

In summary, the observation of a large TMR in hybrid

$\text{MnAs}/\text{AlAs}/\text{Ga}_{1-x}\text{Mn}_x\text{As}$ magnetic tunnel junctions indicates an excellent model system for studying spin injection from a ferromagnetic metal into a semiconductor. Even with conservative estimates for the spin polarization in the ferromagnetic layers, this observation indicates highly efficient spin injection through the AlAs barrier. Modeling of the I - V characteristics at temperatures above the Curie temperature of the $\text{Ga}_{1-x}\text{Mn}_x\text{As}$ layer allow us to understand the nature of the barrier in great detail.

N.S., S.H.C. and K.C.K. were supported by Grant Nos. ONR N00014-99-1-0071, -0716, and DARPA/ONR N00014-99-1-1093. P.S. and S.P. were supported by Grant Nos. DARPA N00014-00-1-0951 and NSF DMR 01-01318. We thank D. D. Awschalom and M. Flatte for a critical reading of this manuscript.

*Electronic address: schun@psu.edu

†Electronic address: nsamarth@psu.edu

¹G.A. Prinz, *Science* **282**, 1660 (1998).

²*Semiconductor Spintronics and Quantum Computation*, 1st ed, edited by D.D. Awschalom, D. Loss, and N. Samarth (Springer-Verlag, Berlin, 2002).

³G. Schmidt *et al.*, *Phys. Rev. B* **62**, R4790 (2000).

⁴Y. Ohno *et al.*, *Nature (London)* **402**, 790 (1999); R. Fiederling *et al.*, *ibid.* **402**, 787 (1999).

⁵A.T. Hanbicki *et al.*, *Appl. Phys. Lett.* **80**, 1240 (2002).

⁶E.I. Rashba, *Phys. Rev. B* **62**, R16267 (2000).

⁷J.S. Moodera, L.R. Kinder, T.M. Wong, and R. Meservey, *Phys. Rev. Lett.* **74**, 3273 (1995).

⁸S. Sugahara and M. Tanaka, *Appl. Phys. Lett.* **80**, 1969 (2002).

⁹M. Tanaka and Y. Higo, *Phys. Rev. Lett.* **87**, 026602 (2001).

¹⁰J.J. Berry *et al.*, *Phys. Rev. B* **64**, 052408 (2001).

¹¹S.J. Potashnik *et al.*, *Appl. Phys. Lett.* **79**, 1495 (2001).

¹²S.H. Chun *et al.*, *Appl. Phys. Lett.* **78**, 2530 (2001).

¹³M. Julliere, *Phys. Lett. A* **54**, 225 (1975); note the difference of

the sign in the denominator because of our choice of normalization resistance.

¹⁴T. Ogawa, M. Shirai, N. Suzuki, and I. Kitagawa, *J. Magn. Magn. Mater.* **196-197**, 428 (1999).

¹⁵S. Sanvito (private communication).

¹⁶S.J. Potashnik *et al.*, *Phys. Rev. B* **66**, 012408 (2002).

¹⁷J.-H. Park *et al.*, *Phys. Rev. Lett.* **81**, 1953 (1998).

¹⁸W.F. Brinkman, R.C. Dynes, and J.M. Rowell, *J. Appl. Phys.* **41**, 1915 (1970).

¹⁹W. Van Roy *et al.*, *J. Cryst. Growth* **227-228**, 852 (2001).

²⁰S. Nemeth *et al.*, *J. Cryst. Growth* **227-228**, 888 (2001).

²¹B.L. Altshuler and A.G. Aronov, *Solid State Commun.* **30**, 115 (1979).

²²W.L. McMillan, *Phys. Rev. B* **24**, 2739 (1981).

²³A similar behavior has been found in metallic and manganese-based MTJs; see E.R. Nowak *et al.*, *Thin Solid Films* **377-378**, 699 (2000); J. O'Donnell *et al.*, *Appl. Phys. Lett.* **76**, 1914 (2000).

²⁴R.C. Dynes and J.P. Garno, *Phys. Rev. Lett.* **46**, 137 (1981).